

Supporting Information

Construction of Fe, N, S- codoped ultra-thin carbon nanosheet superstructure for oxygen reduction reaction

Yu Wang, Ningning Guo, Liangkui Zhu, Ying Pan, Runwei Wang*, Zongtao Zhang and Shilun Qiu

State Key Laboratory of Inorganic Synthesis and Preparative Chemistry,

Jilin University,

Changchun 130012, PR China.

E-mail: rwwang@jlu.edu.cn

Experimental Section

Synthesis of Fe NS-PCs.

2-Aminophenyl disulfide (0.2g) was dissolved in 50mL ethanol, and stirred under room temperature for 30 min. x g (x=1, 2 or 3) $\text{FeCl}_3 \cdot 6\text{H}_2\text{O}$ was then added to form clear solution. After stirred for another 12h, the clear solution transform into dark viscous mixture. Ethanol and water was removed on the rotary evaporator. The product was further dried under 150 °C for at least 8h. the obtained solid product was grinded and carbonized under desired temperature for 1h with a heating rate of 5°C min⁻¹ to yield FeNS-Cs. FeNS-Cs was soaked in 3 M HCl for 24 h, washed with excess deionized water until the residue solution achieve neutral pH. Then the products were washed with ethanol, isolated by centrifugation and dried under 80 °C overnight.

Table S1 Details of synthetic parameter

Sample name	$\text{FeCl}_3 \cdot 6\text{H}_2\text{O}$ (g)	Carbonization temperature(°C)
FeNS/PC-900	2	900
FeNS/PC-800	2	800
FeNS/PC-700	2	700
FeNS/PC-600	2	600
FeNS/PC-800-1	1	800
FeNS/PC-800-3	3	800

Characterization

Powder XRD patterns were obtained by using a Rigaku 2550 diffractometer with Cu Ka radiation ($\lambda = 0.15418$ nm). TG-MS was performed on NETZSCH STA499F3 QMS403D\Bruker V70 under N_2 atmosphere at a heating rate of 10 °C min^{-1} . Scanning electron microscopy (SEM) was done on a Hitachi S-5200 electron microscope. Transmission electron microscopy (TEM) images were obtained on an FEI Tecnai G2 F20s-twin D573 field emission transmission electron microscope at an accelerating voltage of 200 kV. N_2 adsorption-desorption isotherms were collected at 77 K on a Micromeritics ASAP 2020 sorptometer. The samples were degassed at 200 °C for a minimum of 10 h prior to analysis. The Brunauer-Emmett-Teller (BET) surface area was calculated using the N_2 adsorption isotherm data in the relative pressure range 0.05 to 0.25 . Total pore volume was obtained at a relative pressure of 0.995 . Micropore volume was determined following the t-plot method. The pore size distributions (PSDs) were obtained from the N_2 adsorption isotherms using the BJH method. The IR spectra were recorded on a Bruker IFS 66 V/S FTIR spectrometer. X-ray photoelectron spectroscopy (XPS) spectra were acquired using an ESCALAB250 spectrometer. Raman spectroscopy was obtained from LabRAM HR Evolution.

Electrochemical measurements

The electrochemical measurements were conducted on a Bio-Logic VSP electrochemical workstation with a standard three-electrode system. A catalyst-coated glassy carbon rotating disk electrode (diameter 3 mm) was used as the working electrode, Ag/AgCl electrode (in 3.5 M KCl solution) and Pt foil were used as the reference and counter electrodes, respectively. To prepare the working electrode, the as-synthesized catalyst (4 mg) was dispersed in a solution of ethanol (0.98 mL) and Nafion suspension (5 wt%, 0.02 mL) under sonication for 2 h to form a homogeneous catalyst ink. Then, the catalyst ink (0.007 mL) was placed drop wise onto a glassy carbon rotating disk electrode and dried in air. Cyclic voltammetry (CV) measurements were carried out in N_2 - or O_2 -saturated 0.1 M KOH solution at a scan rate of 50 mV s^{-1} . The rotating disk electrode (RDE) tests were performed in O_2 -saturated 0.1 M KOH solution at a sweep rate of 5 mV s^{-1} . All the electrochemical measurements were performed at room temperature. For comparison, the same electrochemical tests with same loading were conducted with commercial Pt/C (20 wt% platinum, Johnson Matthey).

The Koutecky-Levich (K-L) plots (J^{-1} vs $\omega^{1/2}$) were analyzed at various electrode potentials. The electron transfer numbers for the oxygen reduction reaction were determined from the slopes of the linear lines according to the K-L equation (Eqn. 1):

$$\frac{1}{J} = \frac{1}{J_L} + \frac{1}{J_K} = \frac{1}{B\omega^{1/2}} + \frac{1}{J_K} \quad (1)$$

$$B = 0.62nFC_0(D_0)^{2/3}\nu^{-1/6} \quad (2)$$

$$J_K = nFkC_0 \quad (3)$$

where J is the measured current density, J_k and J_L are the kinetic- and diffusion-limited current densities, ω is the angular velocity of the disk ($\omega = 2\pi N$, N is the rotation speed), n is the electron transfer number, F is the Faraday constant ($F = 96485 \text{ C mol}^{-1}$), C_0 is the bulk concentration of O_2 ($C_0 = 1.2 \times 10^{-6} \text{ mol cm}^{-3}$ in 0.1 M KOH), D_0 is diffusion coefficient of O_2 ($D_0 = 1.9 \times 10^{-5} \text{ cm}^2 \text{ s}^{-1}$ in 0.1 M KOH), ν is the kinematic viscosity of the electrolyte ($\nu = 0.01 \text{ cm}^2 \text{ s}^{-1}$ in 0.1 M KOH), and k is the electron transfer rate constant.

The electron transfer number and the peroxide percentage can be calculated by the following equations:

$$n = 4 \times \frac{I_d}{I_r/N + I_d}$$

(4)

$$\%HO_2^- = 200 \times \frac{I_r/N}{I_r/N + I_d}$$

(5)

Here, I_d and I_r are the disk and ring currents, respectively, and $N=0.424$ is the ring collection efficiency.

For stability tests, chronoamperometric measurements were conducted at -0.3 V (vs. Ag/AgCl) at a rotating speed of 1600 rpm in O_2 -saturated 0.1 M KOH solution. The measured potentials against Ag/AgCl were converted to RHE using the relation, $E_{\text{potential vs. RHE}} = E_{\text{potential vs. Ag/AgCl}} + 0.2046 \text{ V} + 0.0592\text{pH}$

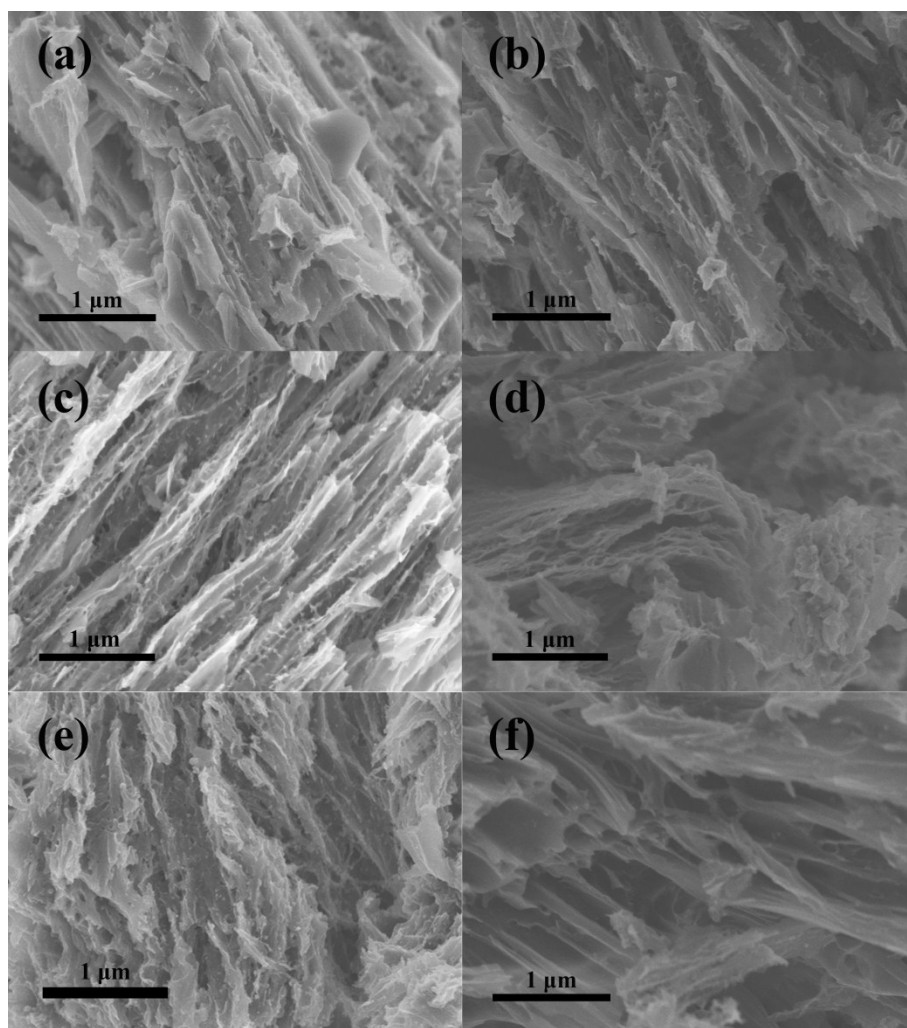


Fig S1, SEM images for (a) FeNS/PC-600, (b) FeNS/PC-700, (c) FeNS/PC-800, (d) FeNS/PC-900, (e) FeNS/PC-800-1 and (f) FeNS/PC-800-3.

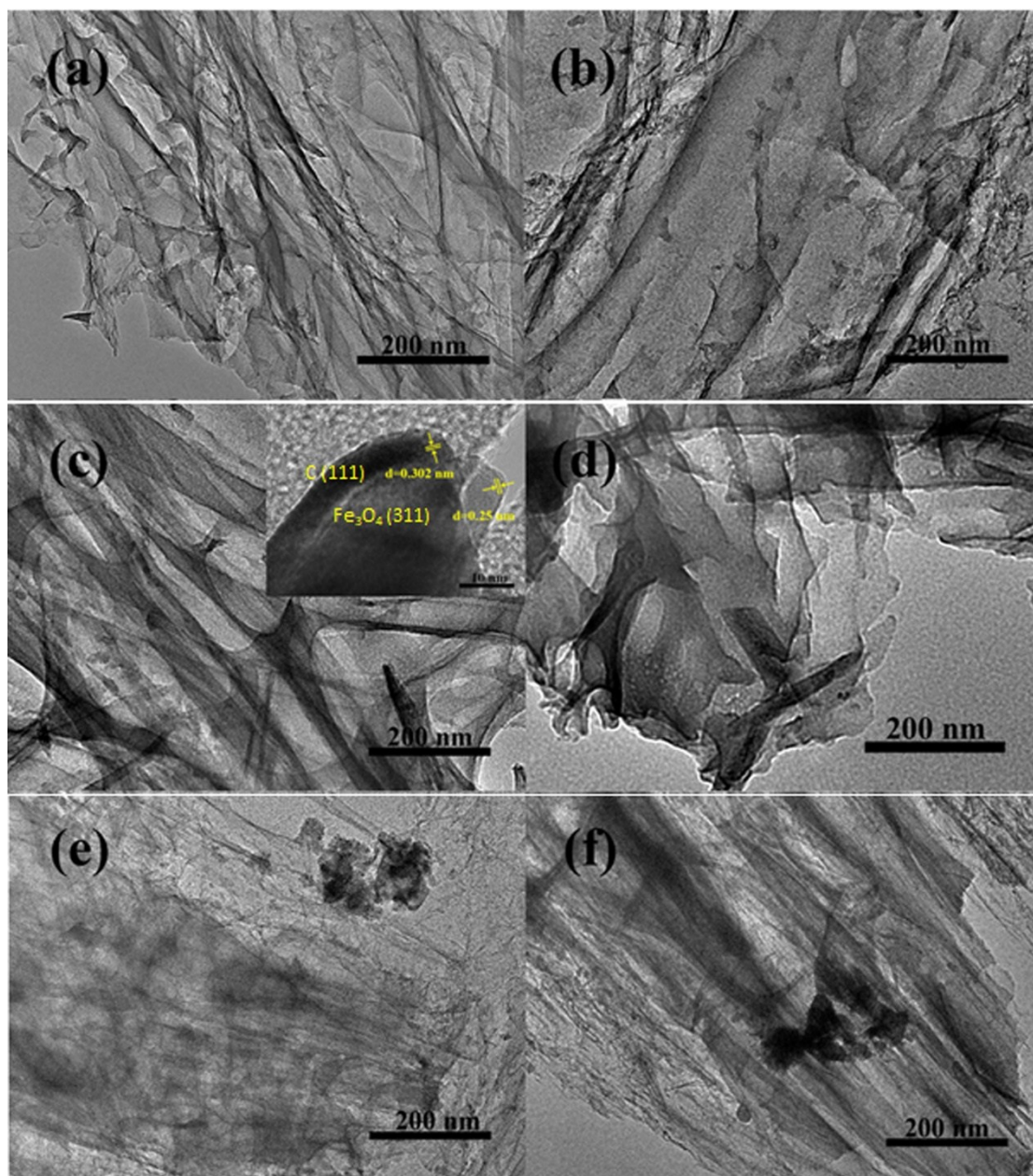


Fig S2, TEM images for (a) FeNS/PC-600, (b) FeNS/PC-700, (c), FeNS/PC-800, (d), FeNS/PC-900, (e) FeNS/PC-800-1 and (f) FeNS/PC-800-3.

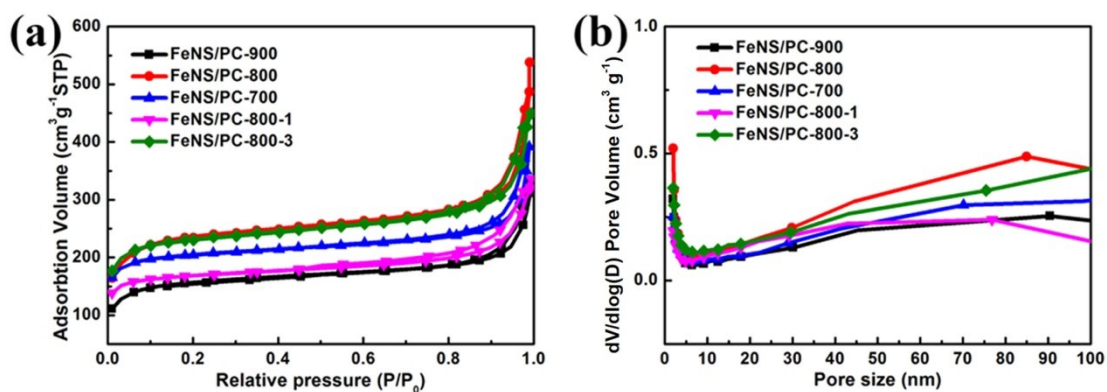


Fig S3, (a) N_2 sorption isotherms for FeNS/PCs, and (b) corresponding BJH pore size distribution.

Table S2, Porosity information for FeNS/PCs.

	S_{BET}	S_{mic}^a	S_{Ext}^b	V_t^c	V_{mic}^a	V_{Ext}^d
	($m^2 \cdot g^{-1}$)	($m^2 \cdot g^{-1}$)	($m^2 \cdot g^{-1}$)	($cm^3 \cdot g^{-1}$)	($cm^3 \cdot g^{-1}$)	($cm^3 \cdot g^{-1}$)
FeNS/PC-900	539	335	204	0.39	0.15	0.24
FeNS/PC-800	816	495	321	0.60	0.22	0.38
FeNS/PC-700	693	520	173	0.46	0.24	0.22
FeNS/PC-800-1	571	429	141	0.42	0.20	0.22
FeNS/PC-800-3	789	542	246	0.56	0.25	0.21

S for surface area ($m^2 g^{-1}$), V for pore volume ($cm^3 g^{-1}$). ^a Micropore volume and micropore area are evaluated by the t-plot method. ^b Mseopore area is determined by subtracting the micropore area from the BET surface area. ^c Total pore volume. ^d Mseopore volume is determined by subtracting the micropore volume from the total pore volume. ^d N content is obtained from element analysis.

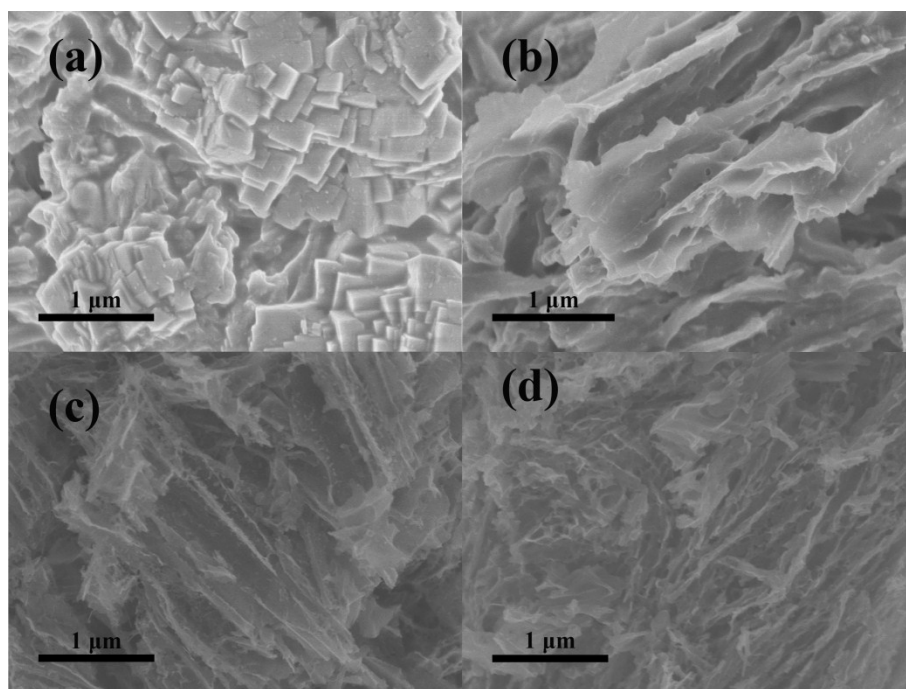


Fig S4, SEM images for (a) FeNS-C-600, (b) FeNS-C-700, (c) FeNS-C-800 and FeNS-C-900.

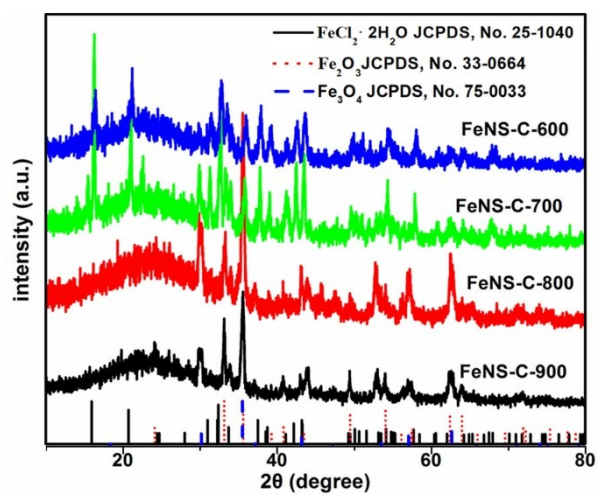


Fig. S5, XRD patterns for FeNS-C-600, FeNS-C-700, FeNS-C-800 and FeNS-C-900.

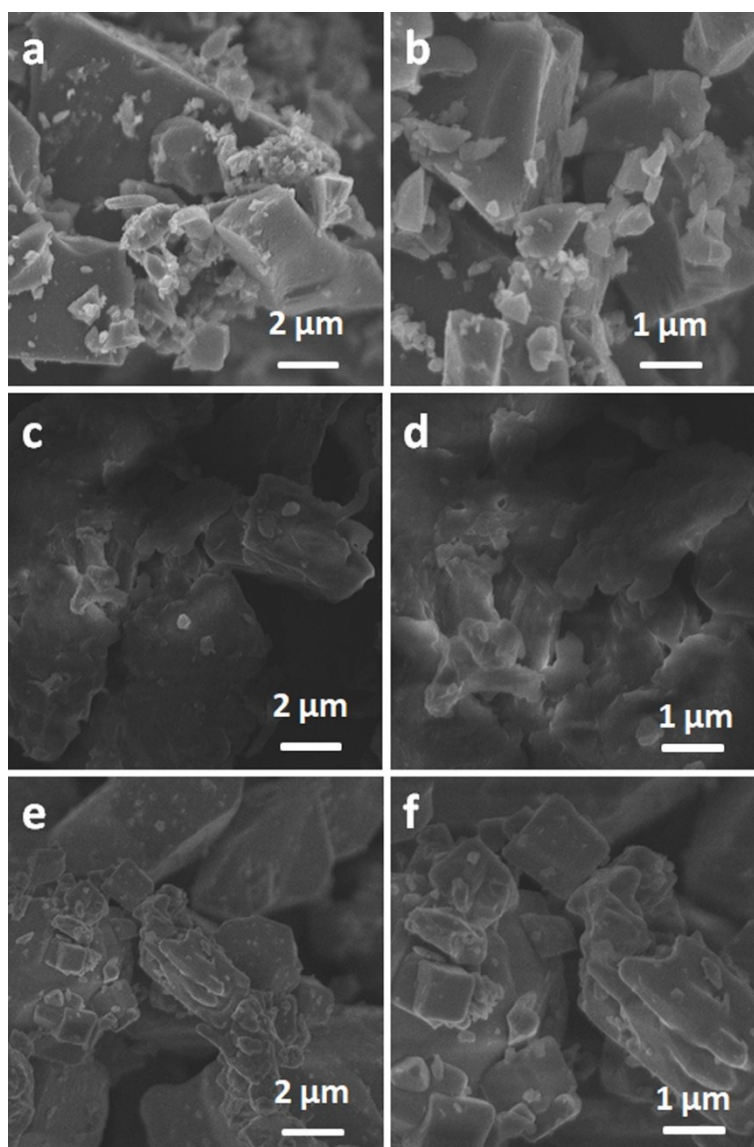


Fig. S6 SEM images for a, b Products for direct calcination of 2-Aminophenyl disulfide; c, d FeCl₃·6H₂O; e, f Products for direct calcination of FeCl₃·6H₂O.

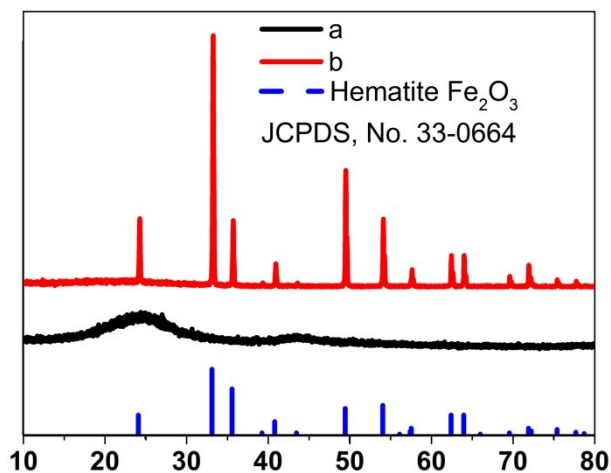


Fig. S7 XRD patterns for samples obtained from a, direct calcination of 2-Aminophenyl disulfide and b, direct calcination of $\text{FeCl}_3 \cdot 6\text{H}_2\text{O}$.

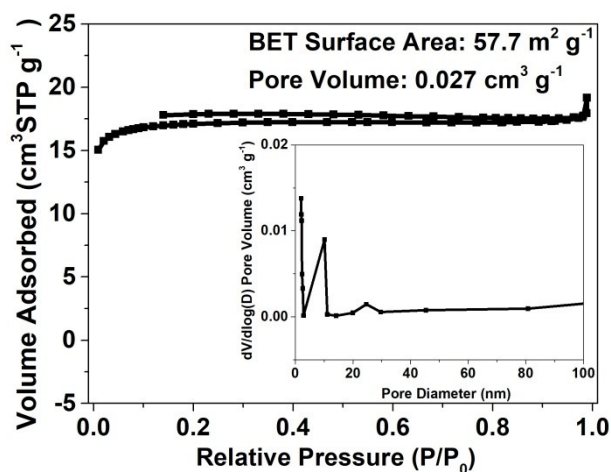


Fig. S8 N_2 sorption isotherms for samples obtained from direct calcination of 2-Aminophenyl disulfide. Insert figure is the corresponding pore size distribution.

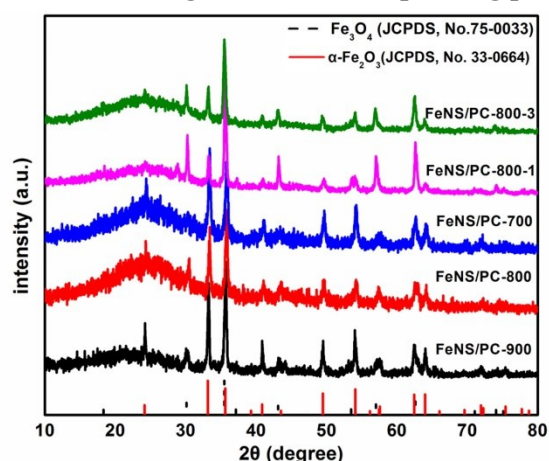


Fig S9, XRD patterns of FeNS/PCs.

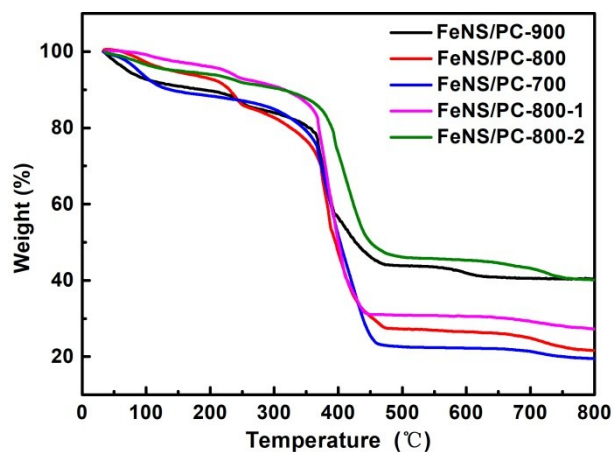


Fig S10, TG results of FeNS/PCs under air atmosphere.

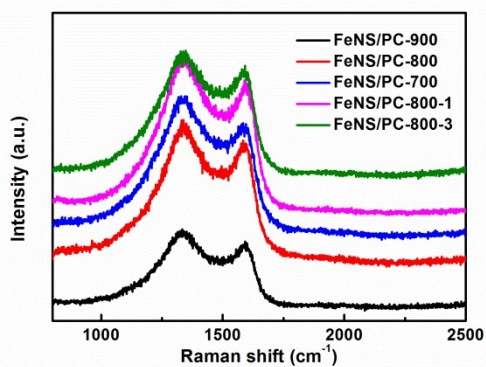


Fig S11. Raman spectrums of Fe NS/PCs.

Table S3. Element analysis results for Fe NS/PCs.

	N (wt%)	S (wt%)
FeNS-PC-900	1.53	11.5
FeNS-PC-800	3.42	15.7
FeNS-PC-700	4.04	6.18
FeNS-PC-1	4.58	9.49
FeNS-PC-3	3.56	8.8

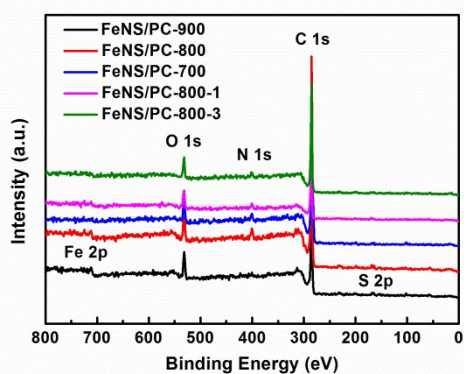


Fig S12 XPS full spectrums for Fe NS/PCs.

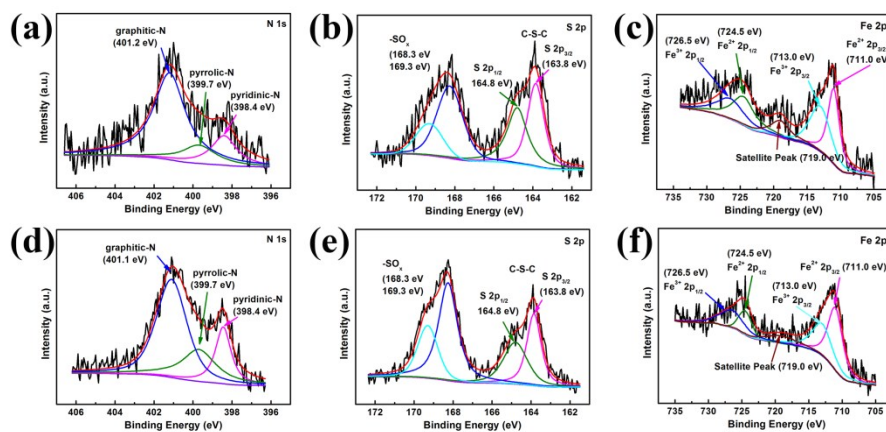


Fig S13 High resolution XPS spectrums for Fe NS/PC-900, (a) N 1s, (b) S 2p and (c) Fe 2p; Fe NS/PC-800, (d) N 1s, (e) S 2p and (f) Fe 2p.

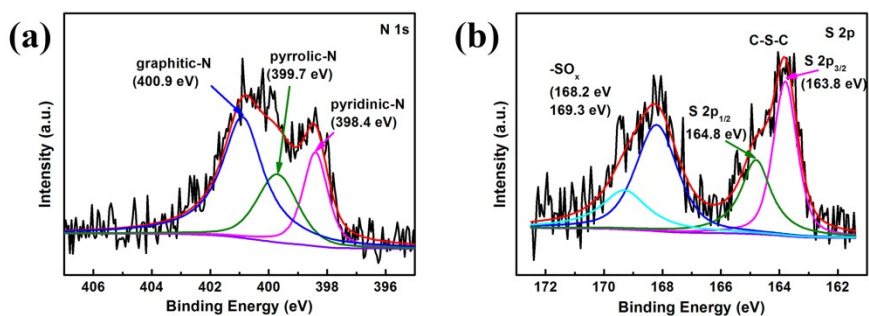


Fig S14 High resolution XPS spectrums for FeNS/PC-700, (a) N 1s, (b) S 2p.

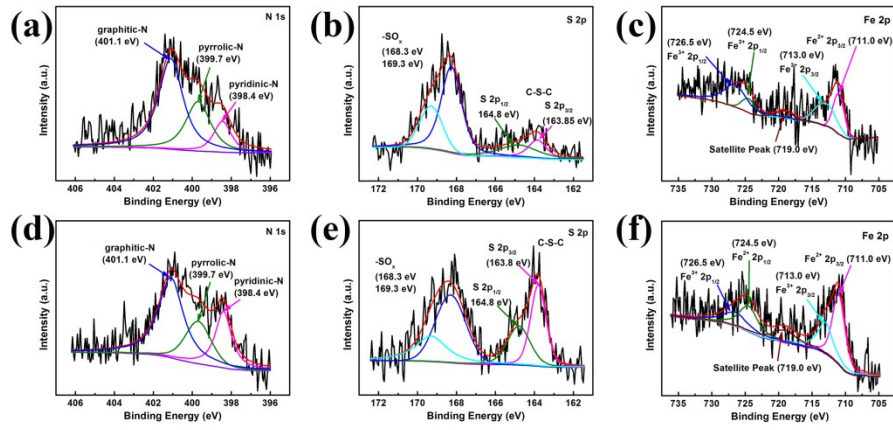


Fig S15 High resolution XPS spectrums for Fe NS/PC-800-1, (a) N 1s,(b) S 2p and (c) Fe 2p; Fe NS/PC-800-3, (d) N 1s, (e) S 2p and (f) Fe 2p.

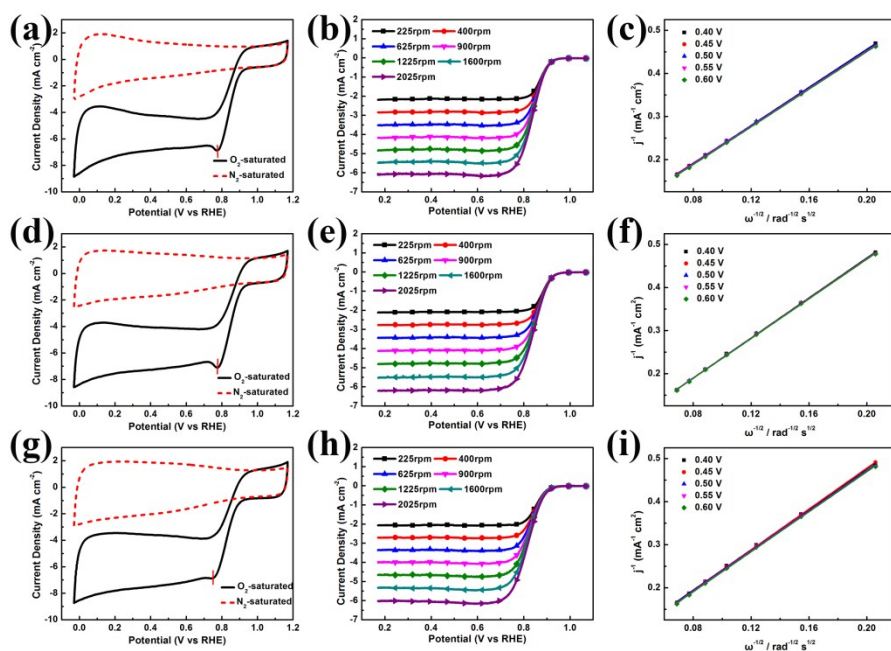


Fig S16 Comparison in ORR activity for FeNS/PCs obtained under different calcination temperature. FeNS/PC-900, (a) CV curves, (b) LSV curves and (c) K-L plots; FeNS/PC-800, (d) CV curves, (e) LSV curves and (f) K-L plots; FeNS/PC-700, (g) CV curves, (h) LSV curves and (i) K-L plots.

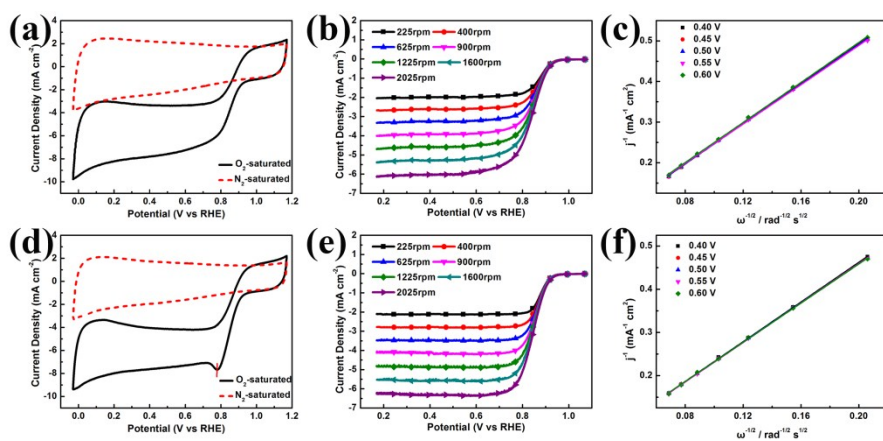


Fig S17 Comparison in ORR activity for Fe NS/PCs obtained with different $\text{FeCl}_3 \cdot 6\text{H}_2\text{O}$ amount. Fe NS/PC-800-1, (a) CV, (b) LSV and (c) K-L; Fe NS/PC-800-3, (d) CV, (e) LSV and (f) K-L.

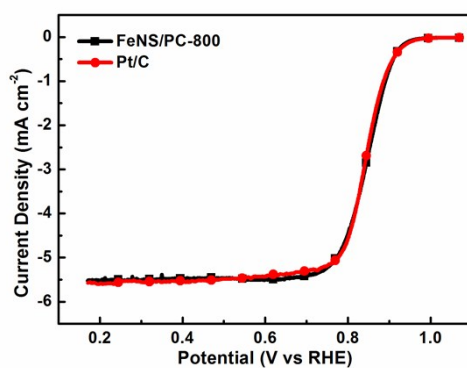


Fig S18 Comparison in ORR activity between Fe NS/PC-800 and 20% Pt/C.

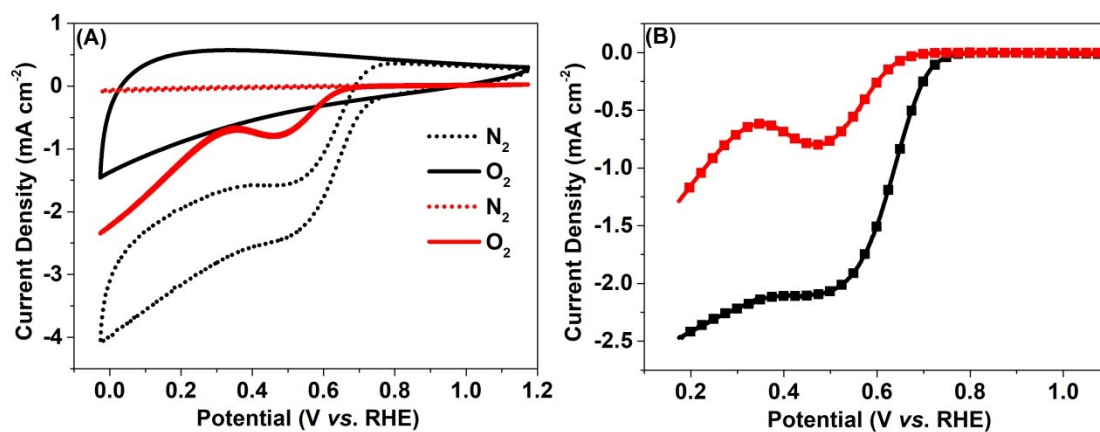


Fig S19 CV curves (A) and LSV curves (B) obtained from direct calcination of 2-Aminophenyl disulfide (black lines) and $\text{FeCl}_3 \cdot 6\text{H}_2\text{O}$ (red lines).

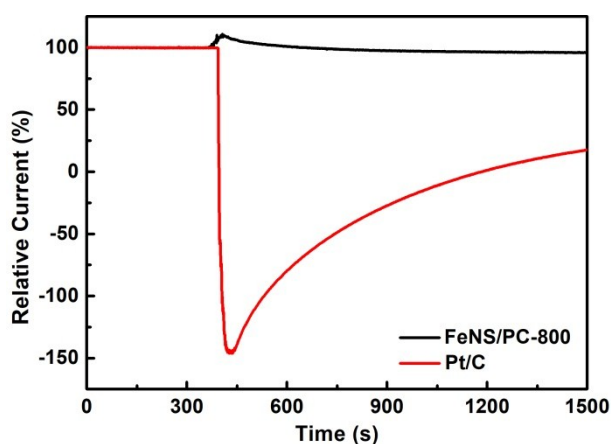


Fig S20 Methanol tolerance tests with 20 wt% Pt/C and RZ9. *I-t* Chronoamperometric response after involving of 3 M methanol.

Table S4 Detail comparison in ORR activity for FeNS/PCs.

	Onset potential (E_{onset} , V)	Half wave potential ($E_{1/2}$, V)	Limiting current (mA cm^{-2})
FeNS-PC-900	0.93	0.84	5.48
FeNS-PC-800	0.95	0.85	5.53
FeNS-PC-700	0.92	0.82	5.32
FeNS-PC-1	0.95	0.84	5.38
FeNS-PC-3	0.94	0.85	5.53